

Engineering Analysis of Tricuspid Annular Dynamics in the Beating Ovine Heart

MANUEL K. RAUSCH,^{1,2,3} MARCIN MALINOWSKI,^{4,5} PENNY WILTON,⁴ ASGHAR KHAGHANI,⁴
and TOMASZ A. TIMEK⁴

¹Department of Aerospace Engineering and Engineering Mechanics, University of Texas at Austin, 210 E 24th Street, WRW Building, Room 305b, Austin, TX 78712, USA; ²Department of Biomedical Engineering, University of Texas at Austin, Austin, TX, USA; ³Institute for Computational Engineering and Sciences, University of Texas at Austin, Austin, TX, USA; ⁴Meijer Heart and Vascular Institute at Spectrum Health, Michigan, MI, USA; and ⁵Department of Cardiac Surgery, Medical University of Silesia, Katowice, Poland

(Received 10 August 2017; accepted 10 November 2017; published online 14 November 2017)

Associate Editor Ender A. Finol oversaw the review of this article.

Abstract—Functional tricuspid regurgitation is a significant source of morbidity and mortality in the US. Furthermore, treatment of functional tricuspid regurgitation is suboptimal with significant recurrence rates, which may, at least in part, be due to our limited knowledge of the relationship between valvular shape and function. Here we study the dynamics of the healthy *in vivo* ovine tricuspid annulus to improve our understanding of normal annular deformations throughout the cardiac cycle. To this end, we determine both clinical as well as engineering metrics of *in vivo* annular dynamics based on sonomicrometry crystals surgically attached to the annulus. We confirm that the tricuspid annulus undergoes large dynamic changes in area, perimeter, height, and eccentricity throughout the cardiac cycle. This deformation may be described as asymmetric in-plane motion of the annulus with minor out-of-plane motion. In addition, we employ strain and curvature to provide mechanistic insight into the origin of this deformation. Specifically, we find that strain and curvature vary considerable across the annulus with highly localized minima and maxima resulting in aforementioned configurational changes throughout the cardiac cycle. It is our hope that these data provide valuable information for clinicians and engineers alike and ultimately help us improve treatment of functional tricuspid regurgitation.

Keywords—Functional tricuspid regurgitation, Strain, Curvature, Sonomicrometry, Splines.

INTRODUCTION

The tricuspid annulus describes the transition zone between the tricuspid leaflets and the surrounding right-sided myocardium.³⁵ Similarly to the mitral annulus, the tricuspid annulus takes on a complex three-dimensional *in vivo* configuration with peaks and valleys and a non-circular in-plane shape.¹¹ Throughout the cardiac cycle this configuration changes dramatically and it may be assumed that the particular nature of this deformation is critical to the functioning of the valve.¹⁵ In fact, changes in annular configuration, specifically annular height, annular area, and annular eccentricity and changes in their evolution throughout the cardiac cycle, are correlated with dysfunction of the tricuspid valve in the absence of any insults to the valve itself, i.e. functional tricuspid regurgitation.^{29,33,34}

Understanding functional tricuspid regurgitation is important as it is a significant cause of morbidity and mortality in the US. For example, up to 35% of patients with atrial fibrillation as well as roughly half of patients with severe pulmonary hypertension suffer from functional tricuspid regurgitation.^{20,23,37} Furthermore, up to 58% of patients depending on left ventricular assist devices and one in three patients receiving mitral valve replacement show signs of functional tricuspid regurgitation.^{7,30} Additionally, treatment of functional tricuspid regurgitation is suboptimal with recurrence rates as high as 30% beyond 1 year after surgery.^{22,36}

High recurrence rates may, at least in part, be due to our limited understanding of the relationship between

Address correspondence to Manuel K. Rausch, Department of Aerospace Engineering and Engineering Mechanics, University of Texas at Austin, 210 E 24th Street, WRW Building, Room 305b, Austin, TX 78712, USA. Electronic mail: manuel.rausch@utexas.edu

valvular shape and function. Thus, we aim to take another step toward a better understanding of the tricuspid annulus. In contrast to previous analyses that have mostly focused on the shape of the tricuspid annulus only, we are using additional, continuous metrics to describe shape *changes*.⁹ Specifically, our goal is to delineate the normal annular dynamics by means of clinical metrics as well as engineering metrics strain and curvature.^{8,24} We chose these metrics as they provide objective and spatially resolved measures of how the shape of the annulus changes throughout the cardiac cycle.² As such, these metrics may not only provide critically needed mechanistic insight into the normal function of the valve, but may also serve as therapeutic target values during the development of surgical repair techniques as well as tricuspid annular repair devices.

MATERIALS AND METHODS

Surgical Procedure and Experimental Protocol

We performed the following surgical procedure and experimental protocol according to the Principles of Laboratory Animal Care, which was formulated by the National Society for Medical Research, and the Guide for Care and Use of Laboratory Animals prepared by the National Academy of Science and published by the National Institutes of Health. Furthermore, this protocol was approved by our local Institutional Animal Care and Use Committee (IACUC#: 12-05).

We described the animal procedure as well as all administered medications in detail previously.^{18,19} Briefly, we pre-medicate the animals, anesthetize them intravenously, intubate and mechanically ventilate them, and maintain anesthesia. We perform a median sternotomy and prepare the animals for cardiopulmonary bypass. Once we initiate bypass, we arrest the heart, open the right atrium and surgically place nine 2 mm sonomicrometry crystals (Sonometrics Corporation, London, ON, Canada) around the tricuspid annulus as per Fig. 1. Subsequently, we exteriorize the crystal wires through a right atriotomy together with a triple-lumen central catheter, place micromanometer pressure transducers (PA4.5-X6; Konigsberg Instruments, Inc., Pasadena, CA, USA) in the left and right ventricles and exteriorize the catheters through the apex. Finally, we close the atriotomy, remove the cross-clamp from the aorta and wean the animals from cardiopulmonary bypass. Before we collect any marker data (at 128 Hz sampling frequency) under open chest, open pericardium conditions, we recover the animals until hemodynamics are stable and normal. At the end

of the experiment, we euthanize all animals and ensure proper marker placements.

Annular Approximation, Interpolation, and Averaging

We calculate engineering metrics along the tricuspid annulus and throughout the cardiac cycle based on cubic spline-based spatial approximations to discrete sonomicrometry crystal data. Toward this end, we follow an approach we previously applied to the mitral valve annulus and described in detail.²⁷ Briefly, we obtain piecewise cubic splines that minimize the distance to the surgical markers and meet a minimal smoothness requirement by minimizing the following objective function,

$$\sum_{n=1}^9 \|\chi_n - \mathbf{c}_n(s, t)\| + \epsilon \int [\partial_s^2 \mathbf{c}(s, t)]^2 ds, \quad (1)$$

where the first term minimizes the distance between the marker coordinates χ_n and the spline segments $\mathbf{c}_n(s, t)$ in a least-square sense. The second term enforces smoothness of the overall annular representation through the penalty parameter ϵ . The resulting spline is a function of the arc-length parameter and time, s and t , respectively. Based on this procedure, we obtain a continuous and sufficiently smooth mathematical representation of the tricuspid annulus through time with which we can determine spatially and temporarily varying engineering metrics of annular dynamics, see “[Engineering Characterization](#)” section.

Because heart rates and relative lengths of systole and diastole vary between animals while acquisition rates are constant, evolutions of clinical as well as engineering metrics vary between animals in duration and number of time points. Thus, we cannot compute mean evolutions of these data by simple averaging. We solve this problem by dividing the cardiac cycle into

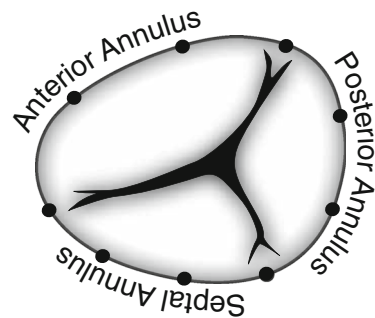


FIGURE 1. Illustration of the tricuspid valve leaflets and annulus with sonomicrometry crystal marker locations. Starting with the antero-septal marker, the average arc-length parameters between consecutive crystals along the annulus at end-diastole are {0,0.11,0.21,0.33,0.43,0.53,0.62,0.72,0.87,1}.

four segments, from end-diastole (ED) to end-isovolumetric contraction (EIVC), from EIVC to end-systole (ES), from ES to end-isovolumetric relaxation (EIVR), and, finally, from EIVR to ED. We identify these four time points in the cardiac cycle as peaks of the QRS complex (ED), the instance of maximum negative left ventricular pressure drop (ES), and as the end-points of the linear segments during isovolumetric contraction and relaxation (as seen in left ventricular pressure recordings), respectively (EIVC, EIVR). Subsequently, we normalize the duration of each segment, linearly interpolate between time points of each segment, scale each segment by the average segment duration between animals, calculate mean segments, and finally re-assemble all segments to obtain average temporal evolutions throughout the cardiac cycle.²⁶

Similar to the temporal averaging above, annuli between animals cannot simply be spatially averaged to obtain a “mean annulus” because reference coordinate systems for the markers vary for each animal. Thus, we first perform a singular value decomposition to determine an optimal rigid transformation that aligns the markers of all animals. Subsequently, we average the marker locations and then perform the same spline approximation on these average marker data as described above.

Clinical Characterization

Annular dynamics are routinely characterized by simple clinical metrics.^{15,16,18} In this tradition, we report tricuspid annular area, tricuspid annular perimeter, annular height, and annular eccentricity to complement engineering metrics. We calculate annular tricuspid area by projecting the spline approximations of the three-dimensional annular configuration onto its best-fit plane. Then, we calculate the inscribed area. Also, based on the same best-fit plane, we calculate the annular height as the plane-normal distance between the most caudal point along the annulus and the most cephalic point. We calculate the tricuspid annular perimeter as the integral of the spline representation along its arc length. Finally, we fit an ellipse to the two-dimensional projection of the tricuspid annular representation. Employing the ellipse’s major and minor axes, we determine the eccentricity of the tricuspid annulus.²⁵ As a reminder to the reader, a circle has an eccentricity of 0, while an ellipse has an eccentricity between 0 and 1. Hence, an increase in eccentricity implies that a shape is becoming more elliptical.

Engineering Characterization

We have described our approach to calculating engineering metrics of annular dynamics before in

detail.^{26,27} Here, we calculate strain and curvature along the tricuspid annulus. Specifically, we calculate Green–Lagrange strain throughout the cardiac cycle as

$$E(s, t) = \left[\lambda(s, t)^2 - 1 \right] / 2, \quad (2)$$

where $\lambda(s, t)$ is the tangential stretch calculated *via*

$$\lambda(s, t) = |\partial_s c(s, t)| / |\partial_s c(s, t_{ED})|. \quad (3)$$

In Eq. (3), we chose the tricuspid annulus at ED as the reference configuration. For the curvature, in addition to reporting absolute values at ED, we also compute relative changes throughout the cardiac cycle by additionally calculating the difference in curvature between the current configuration and the reference configuration at ED according to

$$\Delta\kappa(s, t) = \kappa(s, t) - \kappa(s, t_{ED}), \quad (4)$$

where the absolute curvature is calculated as per

$$\kappa(s, \tau) = |\partial_s c(s, \tau) \times \partial_s^2 c(s, \tau)| / |\partial_s c(s, \tau)|^3. \quad (5)$$

Finally, we compute annular height of each point along the annulus to illustrate the out-of-plane shape and dynamics of the annulus, where we report absolute values (at ED) and relative values. The latter, we calculate by simply subtracting the annular distance from the best-fit plane at each time point from the annular distances in the reference configuration (ED).

Statistics

Unless stated otherwise, we report data as mean \pm 1 standard deviation. Results are compared *via* paired Student’s *t* test with $\alpha = 0.05$.

RESULTS

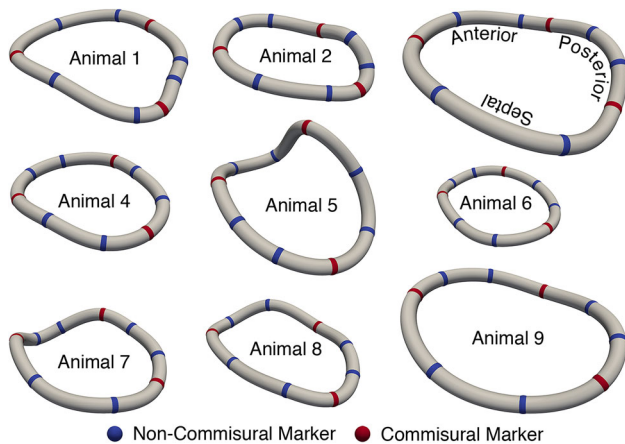
All nine subjects included in our study recovered well from bypass with normal hemodynamics, see Table 1. Also, we successfully acquired and analyzed marker locations for all annular locations and verified their correct placement at the end of our study.

Based on these data we successfully described the annuli of all nine subjects *via* cubic splines throughout one cardiac cycle. The resulting annular configurations for all nine subjects are shown at ED in Fig. 2. We overlay these spline fits with approximated commissural and non-commissural markers to delineate the anterior, posterior, and septal portions of the annulus. Although all nine annuli took on similar three-dimensional configurations, the figure also illustrates inter-subject variations that represent geometric population variances in the context of which the average configurations in Figs. 4 and 5 should later be viewed.

TABLE 1. Hemodynamic data for experimental animals presented as mean \pm 1 standard deviation.

HR (min^{-1})	100 ± 17
RVP ED (mmHg)	12 ± 8
RVP max (mmHg)	31 ± 9
RV ED (ml)	56 ± 10
RV ES (ml)	46 ± 11
LVP ED (mmHg)	19 ± 14
LVP max (mmHg)	111 ± 24
CVP (mmHg)	11 ± 3

HR heart rate, RV right ventricular, RVP right ventricular pressure, LVP left ventricular pressure at ED end-diastole, ES end-systole.

**FIGURE 2. Spline approximations of annuli at end-diastole for all studied animals with approximate commissural and non-commissural marker locations.**

Using the averaging technique described in “[Annular Approximation, Interpolation, and Averaging](#)” section we calculated clinical metrics of tricuspid annular dynamics throughout the cardiac cycle. In Fig. 3, we find that, after a brief delay, tricuspid annular area rapidly decreases after the onset of systole. Additionally, we find that tricuspid annular area reduction begins reversing at mid-systole so that at ES tricuspid annular area has nearly returned to ED values. In the course of diastole, tricuspid annular area continues to increase reaching its peak value around mid-diastole before beginning its descend toward ED values. Not surprisingly, we find the same qualitative trend in tricuspid annular perimeter. In contrast, tricuspid annular height increases starting at ED all the way through about one-third of diastole before it decreases and remains approximately constant for the latter half of diastole. Lastly, tricuspid annular eccentricity undergoes the most marked change of the reported metrics. After a brief drop immediately following ED, eccentricity increases rapidly, i.e. the annulus becomes more elliptical, until the ES, when it drops at a nearly constant rate toward ED values, where the annulus becomes more circular again.

While temporally interpolated evolutions provide insight into average trends of our clinical metrics, peaks in these metrics that are not aligned may be smoothed out. Thus, we also report average peak values in all four metrics, see Table 2.

Figure 4 illustrates mean annular curvature and annular height projected onto the average annulus at ED. The average annulus is approximately elliptically shaped with its major axis extending from the anterior to the posterior-septal aspects of the annulus, where the annular curvature is maximal. It’s out of plane shape is dominated by peaks in annular height at the antero-septal commissure and toward the antero-posterior to mid-posterior segment.

We further illustrate the spatially and temporally varying values of relative height, tangential strain, and relative curvature at EIVC, ES, and EIVR (all relative to ED) in Fig. 5 by projecting their mean values onto the average annular configuration. We find that the annulus takes on a more pronounced out-of-plane configuration with the largest increases in height close to its mid-septal and antero-posterior aspects. Tangential strains reveal mechanistic insight into qualitative trends that we observed in annular area and annular perimeter earlier. Specifically, between ED and EIVC, when the area of the annulus decreases, tangential strains become predominantly negative implying that the annulus contracts (mostly in the anterior and posterior regions). In contrast, at ES and EIVR the annulus partially expands relative to ED mostly driven by changes in the antero-posterior and septal annulus, while the antero-septal region and, to a lesser extent, the posterior region remain contracted. Especially changes in annular eccentricity are explained by variations in relative curvature. We find that curvature increases from ED to EIVC, ES, and EIVR highly focused on the antero-septal region and the postero-septal region, while all other regions become more flat. Thus, the increases in eccentricity and hence the transformation of the annulus into a more elliptical shape, is driven by an in-plane motion of the annulus that hinges at its antero-septal and postero-septal aspects.

DISCUSSION

This is the most detailed engineering analysis of tricuspid annular dynamics in the beating ovine heart to date. In addition to calculating clinical metrics of annular dynamics such as area, perimeter, height, and eccentricity, we also calculated engineering metrics strain and curvature. While the clinical metrics mostly confirm intuitive expectations for temporal changes, our engineering characterization provides mechanistic

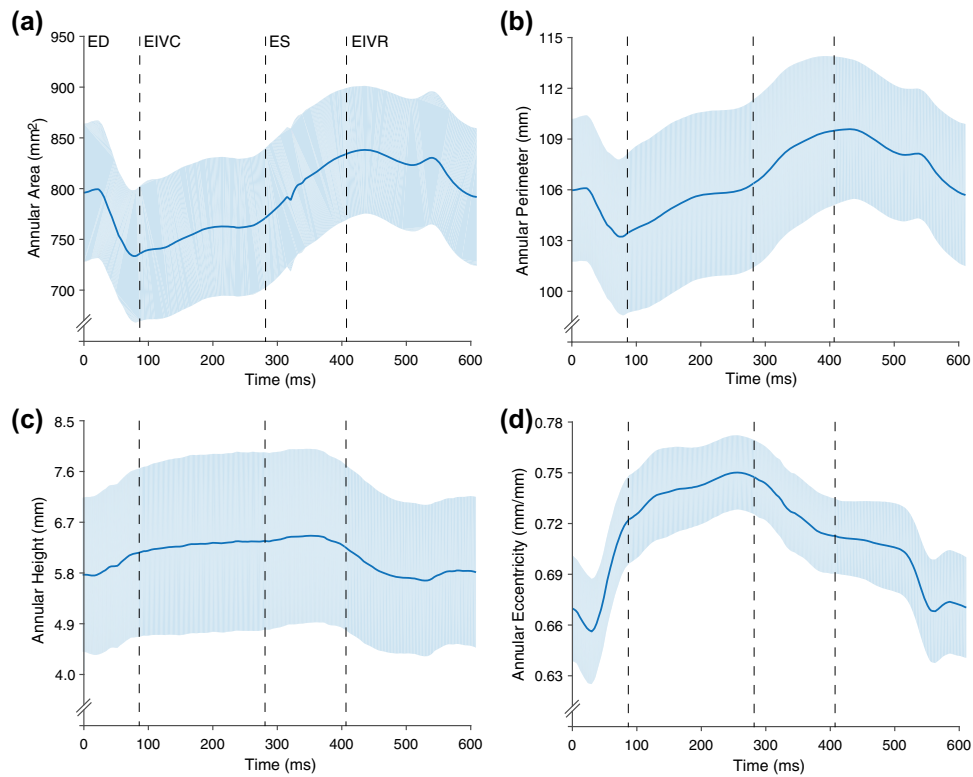


FIGURE 3. Temporally aligned and averaged clinical metrics reported as mean \pm standard error where 0 s coincides with end-diastole. Vertical lines indicated end-isovolumetric contraction (EIVC), end-systole (ES), and end-isovolumetric relaxation (EIVR).

TABLE 2. Clinical metrics of tricuspid annular dynamics.

Annular	Diastole	Systole	Change	p
Area (mm ²)	865.36 \pm 197.67	716.74 \pm 193.17	- 17.53 \pm 7.79%	< 0.001
Perimeter (mm)	111.17 \pm 12.72	102.13 \pm 128.10	- 8.28 \pm 3.49%	< 0.001
Height (mm)	5.33 \pm 4.05	6.55 \pm 4.72	19.70 \pm 12.26%	< 0.01
Eccentricity (-)	0.65 \pm 0.08	0.75 \pm 0.06	13.95 \pm 6.34%	< 0.001

Diastole are the mean peak values of each metric during diastole (maxima of *Area* and *Perimeter*, minima of *Height* and *Eccentricity*), while *Systole* are the mean peak values of each metric during systole (minima of *Area* and *Perimeter*, maxima of *Height* and *Eccentricity*). We calculate *Change* as the percentage change between peak values during diastole and peak values during systole. $p < 0.05$ implies that *Change* is significantly different from 0%.

insight into the origin of these changes. Additionally, we were able to resolve spatial changes along the annulus. Thus, we provide information on the heterogeneity of tricuspid annular deformation.

Clinical Metrics

The dynamic changes of the tricuspid annulus, in terms of clinical metrics, are best described as an asymmetric contraction with in-plane motion and minor out-of-plane motion during systole. This deformation is, qualitatively as well as quantitatively, similar to the deformation of the mitral valve annulus throughout the cardiac cycle. In fact, based on the same approximation technique and similar marker technique, we found dynamic changes in mitral valve annular area, annular height, and eccentricity of

- 14.6, 65.0 and 13.5%, respectively.²⁵ On the other hand, tricuspid annular changes for the same metrics were - 17.5, 19.7, and 14.0% (these results compare favorably to previous findings based on the same technology and animal model with tricuspid annular area and perimeter changes of - 21.9 and 12.5%, respectively¹⁴). Thus, only dynamic changes in annular height vary significantly between the mitral annulus and the tricuspid annulus, possibly due to the tri-leaflet structure of the tricuspid valve likely giving rise to a more complex shape with larger variations.¹

Engineering Metrics

We support our observation on the annular transformation *via* clinical metrics with spatially resolved engineering metrics. Specifically, we find that out-of-

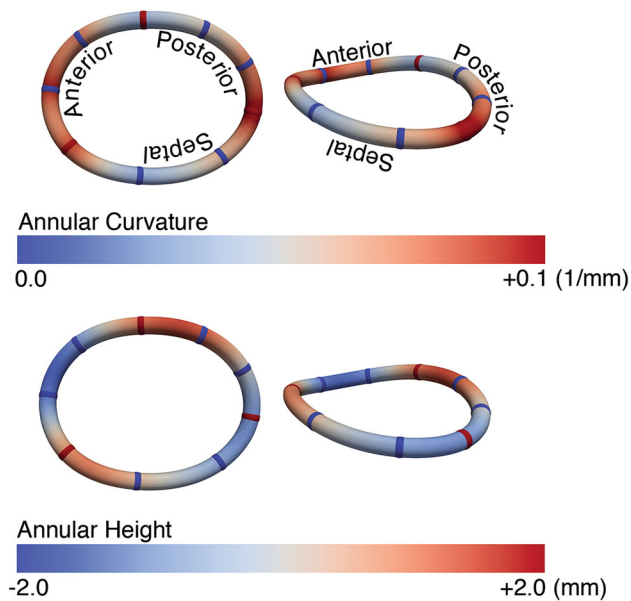


FIGURE 4. Mean values of engineering metrics of annular shape projected onto a spatially aligned and averaged annulus at end-diastole from an atrial view (left) and an isometric view (right).

plane motion of the tricuspid annulus is driven by at least two distinct locations around the annulus. This type of out-of-plane deformation has been shown to be critical to the functioning of the mitral valve by minimizing leaflet tissue stresses.^{1,31,33} Presumably, the tricuspid “saddle” has a similar function on the right side. However, to date, no detailed analysis has been provided to this end. Thus, further study of the tricuspid annular saddle shape may be warranted. We found that the in-plane motion of the tricuspid annulus is governed by asymmetric contraction during systole. Tangential strain and relative curvature seem to imply that this deformation originates from local contractions at the vertices (antero-septally and postero-septally) of the presumed ellipse and slight elongation at the co-vertices (antero-posteriorly and mid-septally). These changes impose an increased curvature in the contractile areas, specifically the vertices, and decreases (flattening) at the co-vertices. Thus, the annulus folds in plane at hinges that approximately coincide with the commissures of the three leaflets.

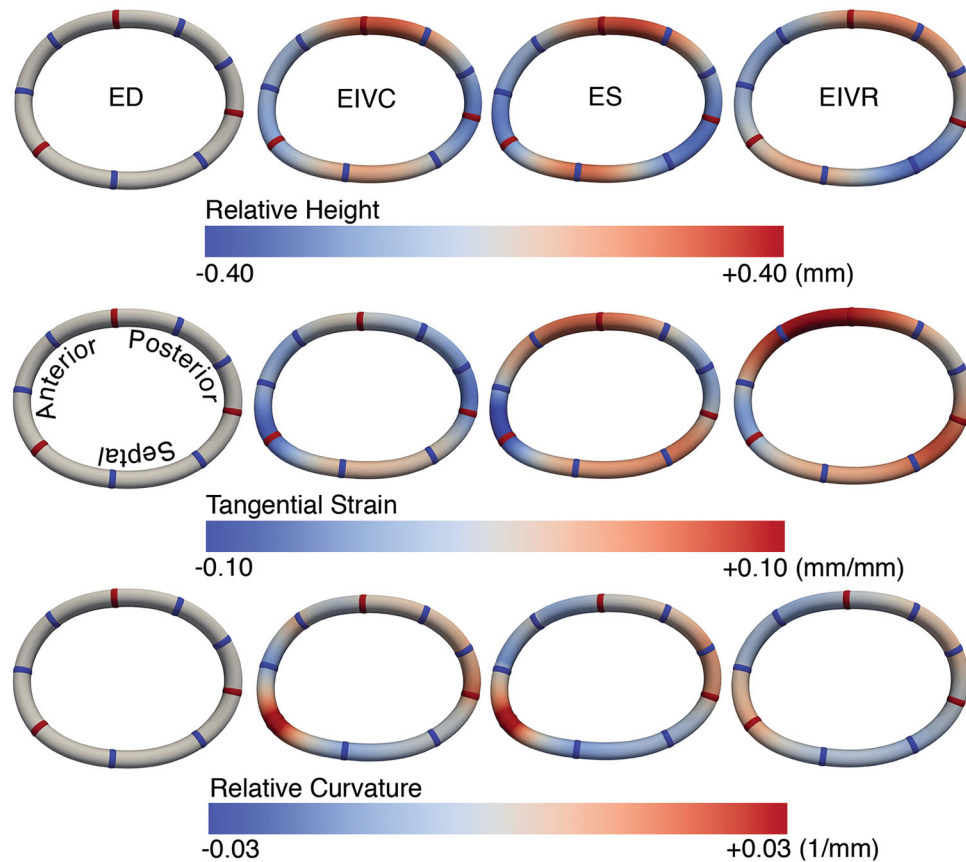


FIGURE 5. Mean values of engineering metrics of annular dynamics projected onto a spatially aligned and averaged annulus at end-diastole (*ED*), end-isovolumetric contraction (*EIVC*), end-systole (*ES*), and end-isovolumetric relaxation (*EIVR*).

Clinical Significance

From a clinical perspective, the importance of our findings may be two-fold. Firstly, we provide the most detailed analysis of the normal *in vivo* dynamics of the tricuspid annulus to date. As such, these data provide a fundamental understanding of what is “normal”. Assuming that the ultimate goal of valve repair and valve replacement is to approximate the healthy valve, detailed knowledge of the healthy annular dynamics is critical to both approaches.¹⁰ To this end, our data may provide target values for surgeons and thus aid in optimizing current repair techniques. Secondly, by providing regionally resolved information on annular dynamics we may help inspire future designs of novel and improved medical devices that accommodate the natural motion of the annulus.^{4,32} On the mitral side, for example, the typical saddle-shape was found to be optimal for minimizing leaflet stresses.³¹ In consequence, a number of medical device manufacturers have developed saddle-shaped annular prostheses or annuloplasty rings.^{3,5,6,28} In this spirit, dynamic data on the deformation of the annulus may inspire more devices that account for the in-plane and out-of-plane motion of the tricuspid annulus with regionally-dependent properties that mimic the “asymmetric contraction with in-plane and minor out-of-plane motion during systole” mentioned above.²¹

Limitations

Of course, this study is not without limitations. Among them, all data were acquired in open-chested animals with open pericardium. Thus, the heart and therefore the tricuspid annulus may be less constraint in our study than under normal conditions. Moreover, we surgically attached sonomicrometry crystals to the annulus whose weight and wire attachments may also affect its normal dynamics. In addition, all animals, necessarily, underwent open-heart surgery prior to data collection. Thus, the valve may have undergone some geometric changes as a result of the surgical intervention. Finally, these data were collected in non-humans. Although, sheep have been used extensively as models for human cardiovascular function and disease, all knowledge derived from our data should be interpreted in this context and with caution.^{12,13,17} On the mathematical side, due to a smoothing term in our objective function our optimized spline functions do not exactly interpolate the marker data collected *in vivo*. However, the choice of our smoothing parameter was based on robustness considerations that were tested on synthetic data with super-imposed noise. Essentially, we argue that large changes in curvature are non-physiological and are due to spurious

motion artifacts and inaccuracies in sonomicrometry crystal data acquisition.

CONCLUSION

We provide the most detailed engineering analysis of tricuspid annular dynamics in the healthy beating ovine heart to date. Our data confirm basic assumptions about annular dynamics, which we believe are best described as an asymmetric contraction with in-plane motion and minor out-of-plane motion. In addition, we compute engineering metrics that provide mechanistic insight into the origin of these motions. Specifically, curvature data and strain data spatially resolve the hinges of these motions as well as areas that dominate annular contraction, respectively. It is our hope that these data will help clinicians and engineers alike in improving our current treatment of functional tricuspid regurgitation.

ELECTRONIC SUPPLEMENTARY MATERIAL

The online version of this article (<https://doi.org/10.1007/s10439-017-1961-y>) contains supplementary material, which is available to authorized users.

ACKNOWLEDGMENTS

This study was supported by an internal Grant from the Meijer Heart and Vascular Institute at Spectrum Health.

CONFLICT OF INTEREST

None of the authors have conflict of interest to report.

REFERENCES

- ¹Amini Khoiy, K., and R. Amini. On the biaxial mechanical response of porcine tricuspid valve leaflets. *J. Biomech. Eng.* 138:104504, 2016.
- ²Amini Khoiy, K., D. Biswas, T. N. Decker, K. T. Asgarian, F. Loth, and R. Amini. Surface strains of porcine tricuspid valve septal leaflets measured in ex vivo beating hearts. *J. Biomech. Eng.* 138:111006, 2016.
- ³Baillargeon, B., I. Costa, J. R. Leach, L. C. Lee, M. Genet, A. Toutain, J. F. Wenk, M. K. Rausch, N. Rebelo, G. Acevedo-Bolton, E. Kuhl, J. L. Navia, and J. M. Guccione. Human cardiac function simulator for the optimal design of a novel annuloplasty ring with a sub-valvular element for correction of ischemic mitral regurgitation. *Cardiovasc. Eng. Technol.* 6:105–116, 2015.

- ⁴Basu, A., and Z. He. Annulus tension on the tricuspid valve: an in-vitro study. *Cardiovasc. Eng. Technol.* 7:270–279, 2016.
- ⁵Bothe, W., E. Kuhl, J. P. E. Kvitting, M. K. Rausch, S. Göktepe, J. C. Swanson, S. Farahmandia, N. B. Ingels, and D. C. Miller. Rigid, complete annuloplasty rings increase anterior mitral leaflet strains in the normal beating ovine heart. *Circulation* 124:S81–S96, 2011.
- ⁶Bothe, W., M. K. Rausch, J. P. E. Kvitting, D. K. Echter, M. Walther, N. B. Ingels, E. Kuhl, and D. Craig Miller. How do annuloplasty rings affect mitral annular strains in the normal beating ovine heart? *Circulation* 126:S231–S238, 2012.
- ⁷Chan, V., I. G. Burwash, B. K. Lam, T. Auyeung, A. Tran, T. G. Mesana, and M. Ruel. Clinical and echocardiographic impact of functional tricuspid regurgitation repair at the time of mitral valve replacement. *Ann. Thorac. Surg.* 88:1209–1215, 2009.
- ⁸Eckert, C. E., B. Zubiato, M. Vergnat, J. H. Gorman, R. C. Gorman, and M. S. Sacks. In vivo dynamic deformation of the mitral valve annulus. *Ann. Biomed. Eng.* 37:1757–1771, 2009.
- ⁹Fawzy, H., K. Fukamachi, C. D. Mazer, A. Harrington, D. Latter, D. Bonneau, and L. Errett. Complete mapping of the tricuspid valve apparatus using three-dimensional sonomicrometry. *J. Thorac. Cardiovasc. Surg.* 141:1037–1043, 2011.
- ¹⁰Fukuda, S., A. M. Gillinov, P. M. McCarthy, W. J. Stewart, J. M. Song, T. Kihara, M. Daimon, M. S. Shin, J. D. Thomas, and T. Shiota. Determinants of recurrent or residual functional tricuspid regurgitation after tricuspid annuloplasty. *Circulation* 114:I-582–I-587, 2006.
- ¹¹Fukuda, S., G. Saracino, Y. Matsumura, M. Daimon, H. Tran, N. L. Greenberg, T. Hozumi, J. Yoshikawa, J. D. Thomas, and T. Shiota. Three-dimensional geometry of the tricuspid annulus in healthy subjects and in patients with functional tricuspid regurgitation a real-time, 3-dimensional echocardiographic study. *Circulation* 2006. <https://doi.org/10.1161/CIRCULATIONAHA.105.000257>.
- ¹²Gorman, J. H., R. C. Gorman, B. M. Jackson, Y. Enomoto, M. G. St. John-Sutton, and L. H. Edmunds. Annuloplasty ring selection for chronic ischemic mitral regurgitation: lessons from the ovine model. *Ann. Thorac. Surg.* 76:1556–1563, 2003.
- ¹³Gorman, J. H., R. C. Gorman, T. Plappert, B. M. Jackson, Y. Hiramatsu, M. G. St. John-Sutton, and L. H. Edmunds, Jr. Infarct size and location determine development of mitral regurgitation in the sheep model. *J. Thorac. Cardiovasc. Surg.* 115:615–622, 1998.
- ¹⁴Hiro, M. E., J. Jouan, M. R. Pagel, E. Lansac, K. H. Lim, H.-S. Lim, and C. M. Duran. Sonometric study of the normal tricuspid valve annulus in sheep. *J. Heart Valve Dis.* 13:452–460, 2004.
- ¹⁵Jouan, J., M. R. Pagel, M. E. Hiro, K. H. Lim, E. Lansac, and C. M. G. Duran. Further information from a sonometric study of the normal tricuspid valve annulus in sheep: geometric changes during the cardiac cycle. *J. Heart Valve Dis.* 16:511–518, 2007.
- ¹⁶Leng, S., M. Jiang, X. D. Zhao, J. C. Allen, G. S. Kassab, R. Z. Ouyang, J. Le Tan, B. He, R. S. Tan, and L. Zhong. Three-dimensional tricuspid annular motion analysis from cardiac magnetic resonance feature-tracking. *Ann. Biomed. Eng.* 44:3522–3538, 2016.
- ¹⁷Malinowski, M., A. G. Proudfoot, D. Langholz, L. Eberhart, M. Brown, H. Schubert, J. Wodarek, and T. A. Timek. Large animal model of functional tricuspid regurgitation in pacing induced end-stage heart failure. *Interact. Cardiovasc. Thorac. Surg.* 24:905–910, 2017.
- ¹⁸Malinowski, M., P. Wilton, A. Khaghani, M. Brown, D. Langholz, V. Hooker, L. Eberhart, R. L. Hooker, and T. A. Timek. The effect of acute mechanical left ventricular unloading on ovine tricuspid annular size and geometry. *Interact. Cardiovasc. Thorac. Surg.* 23:391–396, 2016.
- ¹⁹Malinowski, M., P. Wilton, A. Khaghani, D. Langholz, V. Hooker, L. Eberhart, R. L. Hooker, and T. A. Timek. The effect of pulmonary hypertension on ovine tricuspid annular dynamics. *Eur. J. Cardio-thorac. Surg.* 49:40–45, 2016.
- ²⁰Mutlak, D., D. Aronson, J. Lessick, S. A. Reisner, S. Dabbah, and Y. Agmon. Functional tricuspid regurgitation in patients with pulmonary hypertension: is pulmonary artery pressure the only determinant of regurgitation severity? *Chest* 135:115–121, 2009.
- ²¹Nishi, H., K. Toda, S. Miyagawa, Y. Yoshikawa, S. Fukushima, M. Kawamura, D. Yoshioka, T. Saito, T. Ueno, T. Kuratani, and Y. Sawa. Tricuspid annular dynamics before and after tricuspid annuloplasty- three-dimensional transesophageal echocardiography. *Circ. J.* 79:873–879, 2015.
- ²²Onoda, K., F. Yasuda, M. Takao, T. Shimono, K. Tanaka, H. Shimpo, and I. Yada. Long-term follow-up after Carpentier-Edwards ring annuloplasty for tricuspid regurgitation. *Ann. Thorac. Surg.* 70:796–799, 2000.
- ²³Oren, M., O. Oren, A. Feldman, L. Bloch, and Y. Turge-man. Permanent lone atrial fibrillation and atrioventricular valve regurgitation: may the former lead to the latter? *J. Heart Valve Dis.* 23:759–764, 2014.
- ²⁴Rausch, M. K., W. Bothe, J. P. E. Kvitting, S. Göktepe, D. Craig Miller, and E. Kuhl. In vivo dynamic strains of the ovine anterior mitral valve leaflet. *J. Biomech.* 44:1149–1157, 2011.
- ²⁵Rausch, M. K., W. Bothe, J. P. E. Kvitting, J. C. Swanson, N. B. Ingels, D. C. Miller, and E. Kuhl. Characterization of mitral valve annular dynamics in the beating heart. *Ann. Biomed. Eng.* 39:1690–1702, 2011.
- ²⁶Rausch, M. K., W. Bothe, J. P. E. Kvitting, J. C. Swanson, D. C. Miller, and E. Kuhl. Mitral valve annuloplasty: a quantitative clinical and mechanical comparison of different annuloplasty devices. *Ann. Biomed. Eng.* 40:750–761, 2012.
- ²⁷Rausch, M. K., F. A. Tibayan, N. B. Ingels, D. C. Miller, and E. Kuhl. Mechanics of the mitral annulus in chronic ischemic cardiomyopathy. *Ann. Biomed. Eng.* 41:2171–2180, 2013.
- ²⁸Rausch, M. K., A. M. Zöllner, M. Genet, B. Baillargeon, W. Bothe, and E. Kuhl. A virtual sizing tool for mitral valve annuloplasty. *Int. J. Numer. Method Biomed. Eng.* 2017. <https://doi.org/10.1002/cnm.2788>.
- ²⁹Ring, L., B. S. Rana, A. Kydd, J. Boyd, K. Parker, and R. A. Rusk. Dynamics of the tricuspid valve annulus in normal and dilated right hearts: a three-dimensional transoesophageal echocardiography study. *Eur. Heart J. Cardiovasc. Imaging* 13:756–762, 2012.
- ³⁰Saeed, D., T. Kidambi, S. Shalli, B. Lapin, S. C. Malaisrie, R. Lee, W. G. Cotts, and E. C. McGee. Tricuspid valve repair with left ventricular assist device implantation: is it warranted? *J. Heart Lung Transplant.* 30:530–535, 2011.
- ³¹Salgo, I. S., J. H. Gorman, R. C. Gorman, B. M. Jackson, F. W. Bowen, T. Plappert, M. G. St John Sutton, and L. H. Edmunds. Effect of annular shape on leaflet curvature in

- reducing mitral leaflet stress. *Circulation* 106:711–717, 2002.
- ³²Smith, D. Annulus Tension in the Tricuspid Valve: The Effects of Annulus Dilation and Papillary Muscle Movement. *Thesis*. 2012.
- ³³Spinner, E. M., D. Buice, C. H. Yap, and A. P. Yoganathan. The effects of a three-dimensional, saddle-shaped annulus on anterior and posterior leaflet stretch and regurgitation of the tricuspid valve. *Ann. Biomed. Eng.* 40:996–1005, 2012.
- ³⁴Spinner, E. M., S. Lerakis, J. Higginson, M. Pernetz, S. Howell, E. Veledar, and A. P. Yoganathan. Erratum: correlates of tricuspid regurgitation as determined by 3d echocardiography: pulmonary arterial pressure, ventricle geometry, annular dilatation, and papillary muscle displacement. *Circulation* 5:43–45, 2012.
- ³⁵Tei, C., J. P. Pilgrim, P. M. Shah, J. A. Ormiston, and M. Wong. The tricuspid valve annulus: study of size and motion in normal subjects and in patients with tricuspid regurgitation. *Circulation* 66:665–672, 1982.
- ³⁶Ton-Nu, T.-T., R. A. Levine, M. D. Handschumacher, D. J. Dorer, C. Yosefy, D. Fan, L. Hua, L. Jiang, and J. Hung. Geometric determinants of functional tricuspid regurgitation. *Circulation* 114:143–149, 2006.
- ³⁷Zhou, X., Y. Otsuji, S. Yoshifuku, T. Yuasa, H. Zhang, K. Takasaki, K. Matsukida, A. Kisanuki, S. Minagoe, and C. Tei. Impact of atrial fibrillation on tricuspid and mitral annular dilatation and valvular regurgitation. *Circ. J.* 66:913–916, 2002.